Comparative Studies of Carbon Materials Synthesized From Waste as Catalysts for Ozonation of Real Textile Wastewater

Vijay A. Juwar
VNIT: Visvesvaraya National Institute of Technology
AJIT RATHOD (ajitprathod@gmail.com)
Visvesvaraya National Institute of Technology https://orcid.org/0000-0001-6060-1404
Shyam M. Kodape
Visvesvaraya Regional College of Engineering: Visvesvaraya National Institute of Technology

Research Article

Keywords: Activated carbon, Multiwalled carbon nanotubes, Ozonation, •OH exposure, Specific ozone dose

Posted Date: October 1st, 2021

DOI: https://doi.org/10.21203/rs.3.rs-881195/v1

Comparative Studies of Carbon Materials Synthesized from Waste as Catalysts for Ozonation of Real Textile Wastewater

Vijay A. Juwar, Ajit P. Rathod*, Shyam M. Kodape

Chemical Engineering Department, Visvesaraya National Institute of Technology, Nagpur-India 440010

Email:ajitprathod@gmail.com

* Corresponding Author

Abstract

In the present work, evaluation of two catalysts, Activated carbon (AC) synthesized from agricultural waste and Multiwalled carbon nanotubes (MWCNT) synthesized from plastic waste, were done for the ozonation of real textile wastewater using *para*- chloro benzoic acid (*p*-CBA) as a probe compound. The effect of pH and catalyst dose were studied in terms of •OH exposure, Rct, rate of *p*-CBA degradation and ozone degradation. The rate constant for the reaction of organic matter with hydroxyl radicals was determined using competition kinetics. The threshold ozone dose for real textile wastewater was found to be 0.51 gm/gm of TOC. With an increase in specific ozone dose, the rate of *p*-CBA degradation was found to be increasing and has shown a positive effect on •OH exposure and Rct. The increasing pH had shown a positive effect on the rate of degradation and decomposition of *p*-CBA and ozone respectively in the case of AC catalyzed ozonation. A similar trend was observed in the case of MWCNTs catalyzed ozonation. A positive effect of pH was observed on •OH exposure and Rct, in AC as well as MWCNTs catalyzed ozonation. The effect of catalyst loading has shown significant enhancement in *p*-CBA degradation, ozone decomposition, •OH exposure and Rct in both AC as well as MWCNTs catalyzed ozonation. However, MWCNTs have proved better than AC as a catalyst for ozonation in studied experimental parameters.

Key words: Activated carbon, Multiwalled carbon nanotubes, Ozonation, •OH exposure, Specific ozone dose

1 Introduction

Ozone (O_3), a powerful oxidant capable of reacting with organic and inorganic compounds, has been widely applied for water and wastewater treatment (Bielski et al. 1985, Hoigné, 1998). The transformation of organic pollutants with ozone occurs via direct reaction with molecular ozone or with hydroxyl radicals (•OH) resulting from ozone decomposition in water [von Gunten, 2003]. Molecular ozone has a limitation of selectively reacting with organic pollutants having single bonds and aromatics substituted with electron withdrawing groups (Langlais et al. 1991). To overcome the limitation of molecular ozone, advanced

oxidation processes (AOPs) based enhanced formation of •OH radicals have been developed (Glaze et. al.1987). Ozone goes through chain reactions and forms several secondary oxidants, prominently, hydroxyl radical, a strongest and most non selective oxidant in water. It readily attacks most of the organic pollutants and converts them into less complex and less harmful intermediate products (Langlais et. al. 1991). In recent times, catalytic ozonation has proven to be an effective technique for aqueous pollutant degradation (Kasprzyk-Hordern et. al.2003). In 1970, heterogeneous catalytic ozonation was likely presented (Chen et. al.1977). Heterogeneous ozonation offers certain favourable circumstances over homogeneous ozonation, for example, cleaner process, independent of additional stoichiometric reagents (Fan et. al. 2014.). Carbon materials, for example, activated or synthetic carbons, have been considered for catalytic ozonation since the 1990s (Jans and Hoigné 1998). Because of supportive properties of carbon materials like ready at a lower price, availability of several pores structures and no metal leaching from synthetic carbon, these materials turned into an attractive alternative for catalytic ozonation. (Fan et.al.2014). The integrated utilization of ozone and activated carbon (AC) has been widely researched by Jans and Hoine (Jans and Hoigné 1998) to eliminate toxic and low biodegradable compounds from water. The process amalgamates the calibre of high oxidative strength of ozone and transformation of ozone into hydroxyl radicals by AC, which can degrade aqueous organic compounds. Numerous aqueous compounds have been successfully degraded by AC catalyzed ozonation. (Fontanier et al.2005, Rodrguez et al. 2008). Nanostructured carbon materials, for example, nanotubes and nanofibres, have diverse surface properties when contrasted with particulate carbon materials, for example, activated carbon. Carbon nanotubes display a great capacity to adsorb compounds from water. (Chiang and Wu, 2010, Yu et. al.2011) The major limitation of AC in liquid media is the diffusion of solute in its micro pores may be very slow; it can be even more disastrous in aqueous media due to the hydrophobic nature of the carbon surface. In contrast, the mesoporus nature of nanocarbon material facilitates diffusion through pore network. (Job et.al. 2006). In literature, there are a few studies reported on multiwalled carbon nanotube (MWCNT) as a very promising material for catalytic ozonation. MWCNT of commercial grade was used in catalytic ozonation of oxalic acid, (Liu et.al.2009) SMX, (Goncalves et al.2012) bezafibrate (Goncalves et. al.2013) and attrazine (Fan et. al. 2014) successfully.

The hydroxyl radical concentration is a crucial parameter for determination of the reaction rate. Due to the low concentration of hydroxyl radicals, its quantitative measurement is rather difficult. On the contrary, ozone concentration can be measured by several methods. (Langlais et al. 1999) For the prediction of hydroxyl radical concentration, a few computer models have been developed.(Chelkowska et al. 1992) An indirect method, using para chlorobenzoic acid (p-CBA), was developed by Elovitz and von Gunten (Elovitz and Von Gunten 1999). Up to recent times, several studies have been conducted to evaluate the effectiveness of AOPs like O_3+ UV, O_3/H_2O_2, O_3/ H_2O_2/UV in terms of hydroxyl radical generation. Most of the studies used municipal wastewater. (Wert et al. 2009, Lee et al. 2013, Lee et al. 2014, Guo et al.2018, Liu et al. 2019, Liu et al. 2020),hospital wastewater (Lee et. al. 2014) and industrial wastewater (Liu et. al. 2020). Very few studies have evaluated catalytic performance for hydroxyl radical generation. (Ahn et al.2017, Guo et al.2018, Guo

et al.2019, Guo et al.2020). There are no studies reported on evaluation of catalytic performance for hydroxyl radical generation in industrial wastewater. In this study, the textile industry wastewater was used to evaluate the effectiveness of activated carbon and multiwalled carbon nanotubes for hydroxyl radical generation. The effect of different parameters such as catalyst, ozone dose, and pH were studied. The total scavenging rate of hydroxyl radicals was evaluated. This study is an attempt to portray a real time picture of hydroxyl radial generation in industrial wastewater with activated carbon and multiwalled carbon nanotubes.

2 Materials and Method

2.1 Water Sampling

A wastewater effluent sample was collected from the equalization tank of the textile industry near Nagpur district, Maharashtra, India. The sample was used without any dilution or additional filtration prior to ozonation experiments. The sample was kept in a refrigerator at 4^0 C before further usage.

Table 1: Characterization of textile wastewater

2.2 Analytical methods

The ozone concentrations in the stock solution were determined by the indigo method. Concentrations of hydroxyl radicals probe compound *p*-chlorobenzoic acid (*p*-CBA) were determined by high performance liquid chromatography (HPLC) with reverse phase column and UV-Vis wavelength detector.

2.3 Experimental set-up

A fresh ozone stock solution (50-60 mgL^{-1}) was prepared by bubbling ozone gas into a one litre gas washing bottle which was ice cooled and contained demineralised water. The ozone gas was generated using ozone generator (Faraday Ozone, India). The catalyst solutions were prepared in wastewater samples with varying concentrations of catalyst and adjusted to pH 5, 7, 8 and 9 using 0.1 N H_2SO_4 and NaOH. The desired ozone dose was achieved by varying ratios of sample and stock solution. The initial concentration of *p*-CBA was 1 μM.

2.4 Preparation of Activated carbon

Cajanus cajan husk was obtained from the pulse processing industry in Nagpur. It was washed with water and double distilled water to remove dust particles. It was then dried to remove moisture content in a hot air oven at about 110^0C for 8 hrs. It was crushed and sieved so as to get particles in the size range of 50 to 100 μm. Then it was carbonized in a muffle furnace at about 450^0C for 4 hours. It was treated with concentrated hydrochloric acid to remove ash from carbon. The pH was brought to 7 by repeated washing of carbon using distilled water. Then it was dried in a hot air oven at 110^0 C for 8 hrs to remove the moisture content. It was activated by treating it with conc. sulfuric acid at the ration of 1:10 (wt.of

carbon/volume of sulfuric acid) for 10 hrs. The mixture was filtered and the filtrate was repeatedly washed with double distilled water to bring the pH to 7. To remove the moisture content, it was dried in a hot air oven at 110^0C for 4 hrs. Then it was heated in a muffle furnace at 800^0C for 2 hours for activation. The scanning electron microscopy image of activated carbon is shown in fig. 1 and the XRD patterns of AC are as shown in fig. 2. The SEM image of activated carbon (AC) shows a plate-like structure with an average thickness of 1-2 micrometers. The SEM image indicates no specific shape and size of materials, i.e. uneven shape and size distribution. The diameters of MWCNTs range from 15.5-22.5 nm in SEM images. It is difficult to determine the % purity of MWCNTs from SEM image. The catalyst appears at the tip of the MWCNTs. The HRTEM analysis shows well aligned graphene walls of around 25-35 with 2-3 nm inner diameters. The XRD scan of AC corresponds to its SEM image showing a high amount of noise which resembles an uneven size and shape.The XRD peak correspounds with carbon peak 2ɵ= 26.26 (At (002) plane). The smooth curve in the XRD pattern indicates high amorphous material. The XRD patterns show a well resolved peak similar to AC for graphite at 2ɵ = 26.62 and indicates the absence of amorphous carbon and asserts the formation of MWCNTs.

Fourier transform infrared spectroscopy (FTIR) and Brunauer-Emmet-Teller (BET) for surface morphology are available in the literature. (Bhusari et al.2020)

Figure 1: SEM image of Activated carbon

Figure: 2 XRD Pattern for Activated Carbon

2.5 Preparation of Multiwalled carbon nanotubes

The MWCNTs were synthesized from polypropylene (PP) bottles used for packing chemicals. The small pieces of PP at an approximate size of 1cm × 1cm were made from cleaned bottles of PP. The mixture of shredded PP and the desired amount of Ni/Mo/MgO catalyst was taken into a silica crucible covered with a lid and kept in an electrically heated muffle furnace at the desired temperature. The red hot crucible was removed from the furnace after 10 min. and was cooled to room temperature. To remove the catalyst particles, the synthesized MWCNTs were ultrasonicated with concentrated hydrochloric acid for 30 mins. By oxidising MWCNTs in a muffle furnace at 400^0C for 2 hrs, the amorphous carbon in the product was removed. The XRD patterns show a well resolved peak for graphite at 2ɵ = 26.62 which indicates absence of amorphous carbon and asserts formation of MWCNTs. The diameters of MWCNTs range from 15.5-22.5 nm in SEM images. It is difficult to determine the purity of MWCNTs from SEM images. The catalyst appears at the tip of the MWCNTs. The HRTEM analysis shows well aligned graphene walls of around 25-35 with 2-3 nm inner diameters. The preparation and characterization of multiwalled carbon nanotubes is discussed in the literature (Bajad et.al.2015). The BET surface area of MWCNTs is 28.5 Sq.m./gm.

3 Results and Discussions

3.1Ozone and •OH Exposure

The ozone exposures were calculated from the area under the ozone decay curves. (von Gunten and Hoigne 1994). The Indigo method was used to determine the residual ozone. (Bader and Hoigne, 1981). *p*CBA (para-chlorobenzoic acid) is usually used as a probe compound due to its low apparent second order reaction rate constant with ozone (< 0.1 M^{-1} s^{-1}) and its high reaction rate with •OH (5.0×109 M^{-1} s-1)(von Sonntag and von Gunten 2012, Rosenfeldt and Linden 2007) The •OH exposure is calculated by equation 1:

$$\int \bullet\mathrm{OH}\, dt = \frac{\ln[pCBA]_0 - \ln[pCBA]}{k_{\bullet\mathrm{OH,pCBA}}} \quad (1)$$

The Rct represents a dimensionless number comparing the potential for oxidation by •OH to the potential for oxidation by O_3. The Rct value is not just the ratio of •OH exposure to O_3 exposure as shown in equation 2, but it is the ratio of total initiation capacity to total inhibition capacity in a system.(Yong and Lin 2012).

$$\mathrm{Rct} = \frac{\int[\cdot\mathrm{OH}]\mathrm{dt}}{\int[\mathrm{O3}]dt} \quad (2)$$

At different reaction times, the measured concentration in the experimental solutions was calculated. Ozone exposures at specific ozone doses are shown in fig.3A.With increasing specific ozone dose, the ozone exposure increases during ozonation. The ozone exposure was (0.625-3.3)*10^-3 M s for the textile wastewater. At a lower specific ozone dose of 0.3 gm O_3/gm TOC, it was not possible to measure ozone exposure. It seemed that ozone was rapidly decomposed during instantaneous ozone demand (IOD) or consumed by water matrix. At different specific ozone doses, the ozone decay was completed within ≤15 min.

It can be seen from fig.3A, that •OH Exposure increases with an increase in specific ozone dose. It shows a linear relation of ozone exposure and specific ozone dose (R^2=0.94) which is agreement with (Audenaert et.al.2013).The •OH Exposure increased from 0.04*10^-10 to 1.4*10^-10 for an increment of specific ozone dose of 0.5 to 1.5 gm O_3/gm TOC. From the linear regression, it was possible to determine the threshold ozone dose. The intercept of the linear line represents the value of threshold ozone dose, for which little •OH is formed from ozone consumption in wastewater effluent. [Lee et.al.2013] Fig.3B shows the *p*-CBA degradation at different specific ozone doses. The *p*-CBA degradation increased from 5 to 62%, for an increase in specific ozone dose of 0.5 to 1.5 gm O_3/gm TOC. As shown in fig.1B, the *p*-CBA degradation increases from 2% at a specific ozone dose of 0.5 to 51% at a specific ozone dose of 1.5 gm O_3/gm TOC. At higher ozone dose, decreased *p*-CBA concentration indicates that ozone dose is a significant factor influencing •OH exposure. As mentioned in Table 2, Rct value increases about 2.74 times at the highest specific ozone dose when compared with the lowest specific ozone dose. Fig. 3C, shows the effect of specific ozone dose on the rate of *p*-CBA degradation. With an increase in specific ozone dose, the rate of *p*-

CBA degradation increases. When the specific ozone dose was increased from 0.5 to 1.5 gm ozone/ gm TOC, the rate of *p*-CBA degradation was observed to increase from 0.002 to 0.022 min^{-1} i.e. nearly 11 times increment in rate constant was observed. The increased specific ozone dose enhances the availability of ozone, which can be further decomposed in to •OH and promotes *p*-CBA degradation.

Figure 3:(A) Effect of specific ozone dose on ·OH exposure (B) Effect of specific ozone dose on *p*-CBA degradation (C) Effect of specific ozone dose on rate of *p*-CBA degradation

Table 2: Effect of specific ozone dose on Rct, ozone and ·OH Exposure

3.2 Effect of pH on the performance of catalytic ozonation

The value pH plays a vital role in the decomposition of ozone in the aqueous system. In aqueous systems, the chain reaction transforms O_3 into •OH. The pH can accelerate the initiation of the chain reaction. The role of initiator, promoters and inhibitors can be played by several compounds.(Staehelin and Hoigne,1985). The formation of $•O_2^-$ is due to the initiator. The promoters are attributed to the regeneration of $•O_2^-$ ions from hydroxyl radicals and the inhibitor compounds are capable of consuming hydroxyl radicals without regeneration of superoxide anions. The *p*-CBA degradation depends on ozone decomposition. Therefore, *p*-CBA degradation is an indirect measure of ozone decomposition. In the case of AC catalyzed ozonation, an increase in pH level from 5 to 9, observed 25 to 60% increment in *p*-CBA degradation and •OH exposure increased from 5.75*10^-11 to 1.83*10^-10 M.s as shown in Table 3 and fig 4A. The rate constant of *p*-CBA degradation increases from 0.008 to 0.030 min^{-1} depicted in fig. 4B. The MWCNT catalyzed shows a similar trend of an increment in pcba degradation with an increase in pH level. At pH 5, 30% *p*-CBA removal was observed and was increased to 70% at 9 pH and the corresponding increase in •OH exposure was from 7.13*10^-11 to 2.40*10^-10 M.s as shown in fig. 5A and Table 4. Fig.5B shows that, the rate constant for *p*-CBA degradation was increased nearly five times for pH 9 when compared with 5 pH (0.008 to 0.041 min^{-1}). The Rct increment for AC catalyzed ozonation is nearly 29 times i.e. from 1.12*10^-8 to 3.25*10^-7 and in the case of MWCNT catalyzed ozonation, the increment was observed to be nearly 42 times at 9 pH when compared pH level of 5 as shown in Table 3&4 respectively. The positive effect of increasing pH was also observed in the rate of ozone decomposition. Both the catalyst AC and MWNCTs have shown enhancement in ozone decomposition rate constant with increasing pH. In the case of AC, for a change in initial pH from 5 to 9, the corresponding change in ozone decomposition rate is from 0.176 to 0.448 min^{-1}. In the case of MWCNTs, for the same change in pH, decomposition rate changes from 0.163 to 0.491min^{-1} as shown in figures 4C and 5C respectively. Because there are more hydroxyl ions accessible under basic conditions for launching radical chain reactions, changes in pH can have a direct influence on liquid phase chain reactions. As a result, at higher pH levels, liquid phase reactions triggered by OH-may account for the bulk of the produced hydroxyl radicals.

Figure 4: Effect of pH on (A) *p*-CBA degradation of AC catalyzed ozonation (B) rate of *p*-CBA degradation of AC catalyzed ozonation (C) rate of ozone decomposition in AC catalyzed ozonation

Table 3: Effect of pH on Rct , ozone and ·OH Exposure in AC catalyzed ozonation

Figure 5: Effect of pH on (A) *p*-CBA degradation of MWCNTs catalyzed ozonation (B) rate of ozone decomposition of MWCNTs catalyzed ozonation (C) rate of ozone decomposition of MWCNTs catalyzed ozonation

Table 4: Effect of pH on Rct, ozone and ·OH Exposure in MWCNTs catalyzed ozonation

3.3 Effect of catalyst loading

The effect of AC and MWCNTs loading on *p*-CBA degradation is as shown in fig.6A & 6B. The pH was maintained at 9. As the dose of AC increased from 50 to 100 mg, *p*-CBA degradation was observed to increase by 9% and further increment to 200 mg had shown 12 % enhancement in *p*-CBA degradation when compared with 50mg dose as shown in fig.6A. The rate of *p*-CBA degradation was observed to increase with an increment in AC dose as depicted in fig 6C. With a fourfold increase in AC dose, i.e., from 50 to 200 mg, the rate of *p*-CBA degradation was observed to enhance by 1.47% times when compared with the 50 mg dose. The •OH exposure also increases with an increase in AC dose. For increment of AC dose from 50 to 200 mg, the •OH exposure increased from 1.83*10^-10 to 2.54*10^-10. The corresponding increase in Rct was observed from 3.25*10^-7 to 1.51*10^-6 as shown in the table 5.

An increment in MWCNTs dose showed enhanced *p*-CBA degradation, increased •OH exposure and increased Rct. When MWCNTs dose was increased from 50 to 100 mg, *p*-CBA degradation was increased by 4% and further increment of MWCNTs dose to 200 mg resulted in 10% enhancement in *p*-CBA degradation as shown in fig.4B. The rate of *p*-CBA degradation was increased by 1.39 times, for increment of MWCNTs dose from 50 to 200mg, when compared with the 50mg dose as shown in fig.4D. The •OH exposure was increased from 2.4*10^-10 to 3.22*10^-10 for an increment of 50 to 200mg and the corresponding increase in Rct was from 1.497*10-8 to 6.42*10-7 as shown in the table 6.

The ozone decomposition follows pseudo first order kinetics. The rate of ozone decomposition increases with an increase in AC dose. When AC loading was increased from 50 to 100mg, the corresponding increase in ozone decomposition rate constant was found to increase from 0.625 to 1.005 min^{-1} and further increase in AC dose to 200mg had shown an ozone decomposition rate of 1.354 min-1in fig.6E. An increase in MWCNTs dose has shown enhancement in ozone decomposition rate constant. For an increase in MWCNTs dose from 50 to 100 mg, the rate constant of ozone decomposition increases from 0.638 to 1.354 min^{-1}. Further increment in MWCNTs loading to 200mg, did not show any increment in ozone decomposition rate constant as illustrated in fig 4F. The positive effect of catalyst loading in

the case of AC and MWCNTs was observed for % increment of *p*-CBA degradation, rate of *p*-CBA degradation and rate of ozone decomposition. The enhancement in •OH exposure and Rct was also observed with increasing dose of AC and MWCNTs. This is attributed to the fact that an increase in catalyst dose provides a greater number of surface active sites and facilitates decomposition of ozone molecules into hydroxyl radicals.

Figure 6: Effect of catalyst loading on(A) *p*-CBA degradation in AC catalyzed ozonation (B) *p*-CBA degradation of MWCNTs catalyzed ozonation (C) rate of *p*-CBA degradation in AC catalyzed ozonation (D) rate of *p*-CBA degradation in MWCNTs catalyzed ozonation (E) rate of ozone decomposition of in AC catalyzed ozonation (F) rate of ozone decomposition of in MWCNTs catalyzed ozonation

Table 5: Effect of catalyst loading on Rct, ozone and ·OH Exposure in AC catalyzed ozonation

3.4 Determination of rate constant for reaction of organic matter with hydroxyl radicals

The competition kinetic method (Liu et al. 2019) was used to estimate the rate constant of reaction of organic matter with hydroxyl radicals, using *p*-CBA as a probe component and t-butanol as a competitive scavenger

The selected wastewater matrix Ÿ•OH scavenging (k_1) was determined by the steady-stateŸ•OH concentration. The steady-state Ÿ•OH concentration followed equation 3 and 4 (Liu et. 2019):

$$k = k_{OH,pCBA}[\bullet OH]_{ss} \qquad (3)$$

$$[\bullet OH]_{ss} = \frac{\alpha_{OH}}{k_a} \qquad (4)$$

Where, is *p*-CBA apparent rate constant of degradation, is the selected wastewater matrix Ÿ•OH scavenging rate constant, is the Ÿ•OH formation rate. $[\bullet OH]_{ss}$is the steady-state •OH concentration.

Substituting equation 4 into equation 3 and then inverting both sides' results in:

$$\frac{1}{k} = \frac{k_1}{k_{OH,pCBA}\alpha_{OH}} \qquad (5)$$

295 In this study, the major ·OH scavengers during ozone-based AOPs in the water matrix are
296 DOM (dissolved organic matters), nitrite (NO_2^-) and carbonate/bicarbonate (CO_3^{2-}/HCO_3^-).
297 Therefore, the selected wastewater matrix ·OH scavenging rate constant followed equation 5:

$$k_a = k_{OH,DOM}[DOM] + k_{OH,NO_2^-}[NO_2^-] + k_{OH,CO_3^{2-}}[CO_3^{2-}] + k_{OH,HCO_3^-}[HCO_3^-] + k_{OH,pCBA}[pCBA] + k_{OH,t\text{-}BuOH}[t\text{-}BuOH] \quad (6)$$

298 And substituting equation 6 into equation 5 results in:

$$\frac{1}{k} = [t\text{-}BuOH]\frac{k_{OH,t\text{-}BuOH}}{k_{OH,pCBA}\alpha_{OH}} + \frac{k_{OH,DOM}[DOM] + k_{OH,NO_2^-}[NO_2^-] + k_{OH,CO_3^{2-}}[CO_3^{2-}] + k_{OH,HCO_3^-}[HCO_3^-]}{k_{OH,pCBA}\alpha_{OH}} + \frac{k_{OH,pCBA}[pCBA]}{k_{OH,pCBA}\alpha_{OH}} \quad (7)$$

299 Furthermore, *p*-CBA abatement follows pseudo-first-order kinetics.

$$\ln\frac{[pCBA]_t}{[pCBA]_0} = -k \times t \quad (8)$$

Where, $[pCBA]_t$and $[pCBA]_0$ are the concentration of *p*-CBA at time t and zero. As such, k can be determined by means of measurement of *p*-CBA concentration. By plotting $1/k$ as a function of the t-BuOH concentration resulting in $1/k$ and the t-BuOH concentration are first-order linear relationships (Fig.S1):

$$Y = A[t\text{-}BuOH] + B \quad (9)$$

$$Y = \frac{1}{k} \quad (10)$$

$$A = \frac{k_{OH,t\text{-}BuOH}}{k_{OH,pCBA}\alpha_{OH}} \quad (11)$$

$$B = \frac{k_{OH,DOM}[DOM] + k_{OH,NO_2^-}[NO_2^-] + k_{OH,CO_3^{2-}}[CO_3^{2-}] + k_{OH,HCO_3^-}[HCO_3^-]}{k_{OH,pCBA}\alpha_{OH}} + \frac{k_{OH,pCBA}[pCBA] + k_{OH,H_2O_2}[H_2O_2]}{k_{OH,pCBA}\alpha_{OH}} \quad (12)$$

300 Dividing equation 11 by equation 10 results in:

$$k_{OH,DOM} = \frac{1}{[DOM]}\left(\frac{B}{A}k_{OH,t\text{-}BuOH} - k_{OH,NO_2^-}[NO_2^-] - k_{OH,CO_3^{2-}}[CO_3^{2-}] - k_{OH,HCO_3^-}[HCO_3^-] - k_{OH,pCBA}[pCBA]\right) \quad (13)$$

The wastewater effluent samples, which were used to determine the selected wastewater $^{\bullet}OH$ scavenging. The results on scavenging kinetics are shown in Fig.7. The results of slope A and intercept B were2.3×10^6 s and 33.2×10^3 s M^{-1}($R^2\approx 0.987$), respectively. Therefore, the total $^{\bullet}OH$ scavenging rate constant $1.6\times 10^4 s^{-1}$

Figure 7: Competition kinetics plot for determination of the $^{\bullet}OH$ scavenging rate constant

3.5Effect of AC and MWCNT catalyzed ozonation on TOC and COD removal

The effect of AC and MWCNT on COD and TOC removal is as shown in the fig.8A& 8B. The catalyst dose, Ph and ozone dose were optimized as earlier. The catalyst dose for AC was 200 mg/L, for MWCNTs was 100mg/L, pH was maintained at 9 and the specific ozone dose was 1.2 gm of ozone /gm of TOC. It can be inferred from fig. COD removal in the case of MWCNTs is comparatively higher than AC catalyzed ozonation. The TOC removal in the case of MWCNT catalyzed ozonation was observed to be higher when compared with AC catalyzed ozonation.

Figure 8: Effect of AC and MWCNT catalyzed ozonation on (A) COD removal (B) TOC removal

4 Conclusions:

In the catalytic ozonation of textile wastewater, two catalysts were used. Activated carbon was synthesized from agricultural waste and Multiwalled carbon nanotubes were synthesized from plastic waste. The minimum requirement of ozone dose to form hydroxyl radicals was found in terms of specific ozone dose. Hydroxyl radical exposure was found to be increasing with an increased specific ozone dose. The rate of *p*-CBA degradation was observed to increase with increase in specific ozone dose and Rct.

Increasing pH from 5 to 9 had shown significant enhancement in hydroxyl radical exposure, rate of *p*-CBA degradation, Rct and rate of ozone decomposition. This trend was observed in AC as well as MWCNT catalysed ozonation. The MWCNT catalyzed ozonation has shown superior performance when compared with AC catalysed ozonation.

With increase in catalyst loading, the remarkable increment in hydroxyl radical exposure, rate of *p*-CBA degradation, Rct and rate of ozone decomposition were observed. The impact of

catalyst loading was found dominantly positive in case of MWCNT catalysed ozonation. The competition kinetic method was used to estimate the rate constant of reaction of organic matter with hydroxyl radicals, using *p*-CBA as a probe component and t-butanol as a competitive scavenger.

Author contribution: All the authors are responsible for the entire manuscript.

Funding: This study is not supported by any agency.

Data Availability: The datasets used and/or analysed during the current study are available from the corresponding author on reasonable request.

Declarations:

Ethics approval and consent to participate: All authors have approval and consent to participate.

Consent for publication: Not applicable.

Competing interests: The authors declare no competing interests.

References

1. Ahn Y, Oh H, Yoon Y, Kyu Park W, Seok Yang W, Kang J, Effect of graphene oxidation degree on the catalytic activity of graphene for ozone catalysis, Journal of Environmental Chemical Engineering, Volume 5, Issue 4, August 2017, Pages 3882-3894, doi.org/10.1016/j.jece.2017.07.038

2. Audenaert W.T.M., Vandierendonck D., Van Hulle S.W.H., Nopens I., Comparison of ozone and HO induced conversion of effluent organic matter (EfOM) using ozonation and UV/H2O2 treatment, Water Res. 47 (2013) 2387–2398, https://doi.org/ 10.1016/j.watres.2013.02.003.

3. Bader, H.; Hoigne, J. Determination of ozone in water by the´indigo method. Water Res. 1981, 15, 449-456, doi.org/10.1016/0043-1354(81)90054-3

4. Bajad G. S., Tiwari S.K.,Vijayakumar R.P.(2015), Synthesis and characterization of CNTs using polypropylene waste as precursor Materials Science and Engineering B 194,68–77. doi.org/10.1016/j.mseb.2015.01.004

5. Bhusari A.,Mazumdar B.,Rathod A.,Khonde R., (2020), Kinetics of catalyzed esterification of acetic acid with n-butanol using carbonized agro waste., International Journal of Chemical Kinetics, Volume52, Issue7, July , Pages 450-462, doi.org/10.1002/kin.21361

6. Bielski B.H.J., Cabelli D.E.,. Arudi R.L, Ross A.B.,Reactivity of HO2/O2- radicals in aqueous solution, J. Phys. Chem. Ref. Data 14 (4) (1985) 1041–1100. https://doi.org/10.1063/1.555739

7. Chelkowska, K., Grasso, D., Fabian, I., Gordon, G., 1992. Numerical simulations of aqueous ozone decomposition. Ozone Sci. Eng.143349 doi.org/10.1080/01919519208552316.

8. Chen J.W., Hui C., Keiler T., Smith G., Catalytic ozonation in aqueous systems, in: AIChE (Ed.), AIChE Symposium Series, AIChE, New York, pp. 206–212, (1977)
9. Chiang Y.C., Wu P.Y., Adsorption equilibrium of sulfur hexafluoride on multiwalled carbon nanotubes, J. Hazard. Mater. 178,729–738, (2010). doi.org/10.1016/j.jhazmat.2010.02.003

10. Elovitz, M.S., von Gunten, U., 1999. Hydroxyl radical/ozone ratios during ozonation processes. I. The *R*ct concept. Ozone Sci. Eng. 21, 239–260,doi.org/10.1080/01919519908547239.

11. Fan Xiaolei, Restivo João, Órfão José J.M., Pereira Manuel Fernando R., Lapkin Alexei A., The role of multiwalled carbon nanotubes (MWCNTs) in the catalytic ozonation of atrazine, Chemical Engineering Journal 241,66–76, (2014). doi.org/10.1016/j.cej.2013.12.023
12. Fontanier V., Farines V., Albert J., Baig S., Molinier J., Oxidation of Organic Pollutants of Water to Mineralization by Catalytic Ozonation, Ozone Sci. Eng. 27,115–128, (2005) doi.org/10.1080/01919510590925239

13. Goncalves AG, Orfao J J M, Pereira M F R; Catalytic ozonation of bezafibrate promoted by carbon materials. Applied Catalysis B: Environment, 2013;140-141(0):82-91, https://doi.org/10.1016/j.apcatb.2013.03.034

14. Goncalves AG,Orfao JJM, Pereira MFR; Catalytic ozonation of sulfamethaxazole in presence of carbon material: Catalytic performance and reaction pathways; J. Hazad. Mater; 2012239-240(0): 167-74, DOI: 10.1016/j.jhazmat.2012.08.057

15. Guo Y, Zhub S, Wanga B, Huanga J, Denga S, Yua G, Wanga Y, Modelling of emerging contaminant removal during heterogeneous catalytic ozonation using chemical kinetic approaches, Journal of Hazardous Materials 380 (2019) 120888, doi.org/10.1016/j.jhazmat.2019.120888

16. Guoa Y, Zhaoa E, Wangb J, Zhanga X, Huangc H, Yua G, Wang Y, Comparison of emerging contaminant abatement by conventional ozonation, catalytic ozonation, O3/H2O2 and electro-peroxone processes, Journal of Hazardous Materials 389 (2020) 121829, doi.org/10.1016/j.jhazmat.2019.121829.
17. GuoY, Wang H, Wang B, Deng S, Huang J, Yu G, Wang Y, Prediction of micropollutant abatement during homogeneous catalytic ozonation by a chemical kinetic model, Water Research 142 (2018) 383e395, doi.org/10.1016/j.watres.2018.06.019
18. Hoigné J., Chemistry of aqueous ozone and transformation of pollutants by ozonation and advanced oxidation processes, in: J. Hrubec (Ed.), Quality and Treatment of Drinking Water II, Springer Berlin Heidelberg, Berlin, Heidelberg, 1998, pp. 83–141.

406 19. Jans U., Hoigné J., Activated carbon and carbon black catalyzed transformation
407 of aqueous ozone into OH-radicals, Ozone Sci. Eng. 20,67–90, (1998).
408 doi.org/10.1080/01919519808547291
409 20. Job N, Sabatier F, Pirard J P, Leonard A.,Towards the production of carbon xerogels
410 monoliths by optimizing convective drying conditions., Carbon 2006, 44(12):2534-42.
411 doi.org/10.1016/j.carbon.2006.04.031
412 21. Kasprzyk-Hordern B. , Ziółek M. , Nawrocki J., Catalytic ozonation and methods of
413 enhancing molecular ozone reactions in water treatment, Appl. Catal. B Environ. 46
414 (4) (2003) 639–669. DOI: 10.1016/S0926-3373(03)00326-6
415 22. Langlais B. , Reckhow D.A., Brink D.R. , Ozone in Water Treatment: Application
416 and
417 Engineering, AWWA Research Foundation and Lewis Publishers, 1991.
418 23. Langlais, B., Reckhow, D.A., Brink, D.R., 1999. Ozone in Water Treatment:
419 Applications and Engineering. Lewis Publishers, Boca Raton, FL
420 24. Lee Y., Gerrity D., Lee M., Bogeat A.E, Salhi E., Gamage S., Trenholm R.A.,
421 Wert E.C., Snyder S.A., von Gunten U., Prediction of micropollutant elimination
422 during ozonation of municipal wastewater effluents: use of kinetic and water specific
423 information, Environ. Sci. Technol. 47 (2013) 5872–5881, https://doi.org/10.
424 1021/es400781r.
425 25. Lee Y., Gerrity D., Lee M., Bogeat A.E., Salhi E., Gamage S., Trenholm R.A.,
426 Wert E.C., Snyder S.A., von Gunten U., Prediction of micropollutant elimination
427 during ozonation of municipal wastewater effluents: use of kinetic and water specific
428 information, Environ. Sci. Technol. 47 (2013) 5872–5881, https://doi.org/10.
429 1021/es400781r.
430 26. Lee Y., Kovalova L., McArdell C.S., von Gunten U., Prediction of micropollutant
431 elimination during ozonation of a hospital wastewater effluent, Water Res. 64
432 (2014) 134–148, https://doi.org/10.1016/j.watres.2014.06.027
433 27. Liu Z Q, Ma J, Cui Y H, Zhang B P, Effect of ozonation pretretment on the surface
434 properties and catalytic activity of multiwalled carbon nanotube. Applied Catalysis B
435 :Environment,2009, 92(3-4):301-6. doi.org/10.1016/j.apcatb.2009.08.007
436 28. Liu Z, YangY , Shao C, Ji Z, Wang Q, Wang S, Guo Y, Demeestere K, VanHulle S,
437 Ozonation of trace organic compounds in different municipal and industrial
438 wastewaters: Kinetic-based prediction of removal efficiency and ozone dose
439 requirements, Chemical Engineering Journal,Volume 387, 1 May 2020, 123405,
440 doi.org/10.1016/j.cej.2019.123405
441 29. Liu Z., Chys M., Yang Y., Demeestere K., and Van Hulle S., Oxidation of Trace
442 Organic Contaminants (TrOCs) in Wastewater
443 Effluent with Different Ozone-Based AOPs: Comparison of Ozone Exposure and •OH
444 Formation, Ind. Eng. Chem. Res. 2019, 58, 8896-8902,
445 doi.org/10.1021/acs.iecr.9b00293
446 30. Rodrı ´guez A., Rosal R., Perdigon-Melon J.A., Mezcua M., Aguera A., Hernando
447 M.D., Leto n P., Ferna ´ndez-Alba A.R., Garcı ´a-Calvo E., Ozone-based technologies

in water and wastewater treatment, Handbook of Environmental Chemistry, vol. 5 Part S/2, Springer-Verlag, Berlin Heidelberg, Germany, pp. 127–175,(2008)

31. Rosenfeldt E.J., Linden K.G., The ROH,UV Concept to Characterize and the Model UV/H2O2 Process in Natural Waters, Environ. Sci. Technol. 41 (2007) 2548–2553. https://doi.org/10.1021/es062353p

32. Staehelin J., Hoigne J., Decomposition of ozone in water in the presence of organic solutes acting as promoters and inhibitors of radical chain reactions, Environ. Sci. Technol. 19 (12) (1985) 1206–1213 doi.org/10.1021/es00142a012

33. von Gunten, U., 2003. Ozonation of drinking water: part I: oxidation kinetics and product formation. Water Research, 37 (7), 1443e1467. DOI: 10.1016/S0043-1354(02)00457-8

34. Von Gunten, U.; Hoigne, J. Bromate formation during ozonation of bromide-containing waters: Interaction of ozone and hydroxyl radical reactions. Environ. Sci. Technol. 1994, 28, 1234-1242, doi: 10.1021/es00056a009

35. Von Sonntag C., Von Gunten U., Chemistry of Ozone in Water and Wastewater Treatment, IWA Publishing, 2012.

36. Wert, E. C.; Rosario-Ortiz, F. L.; Snyder, S. A. Effect of Ozone Exposure on the Oxidation of Trace Organic Contaminants in Wastewater. Water Res. 2009, 43 (4), 1005-1014. DOI: 10.1016/j.watres.2008.11.050

37. Yong, E.L. and Lin, Y.P., 2012. Incorporation of initiation, promotion and inhibition in the R-ct concept and its application in determining the initiation and inhibition capacities of natural water in ozonation. Water Research 439 46(6), 1990-1998. DOI: 10.1016/j.watres.2012.01.025

38. Yu F., Ma J., Wu Y.Q.,Adsorption of toluene, ethylbenzene and m-xylene on multi-walled carbon nanotubes with different oxygen contents from aqueous solutions, J. Hazard. Mater. 192, 1370–1379, (2011). doi.org/10.1016/j.jhazmat.2011.06.048

Figures

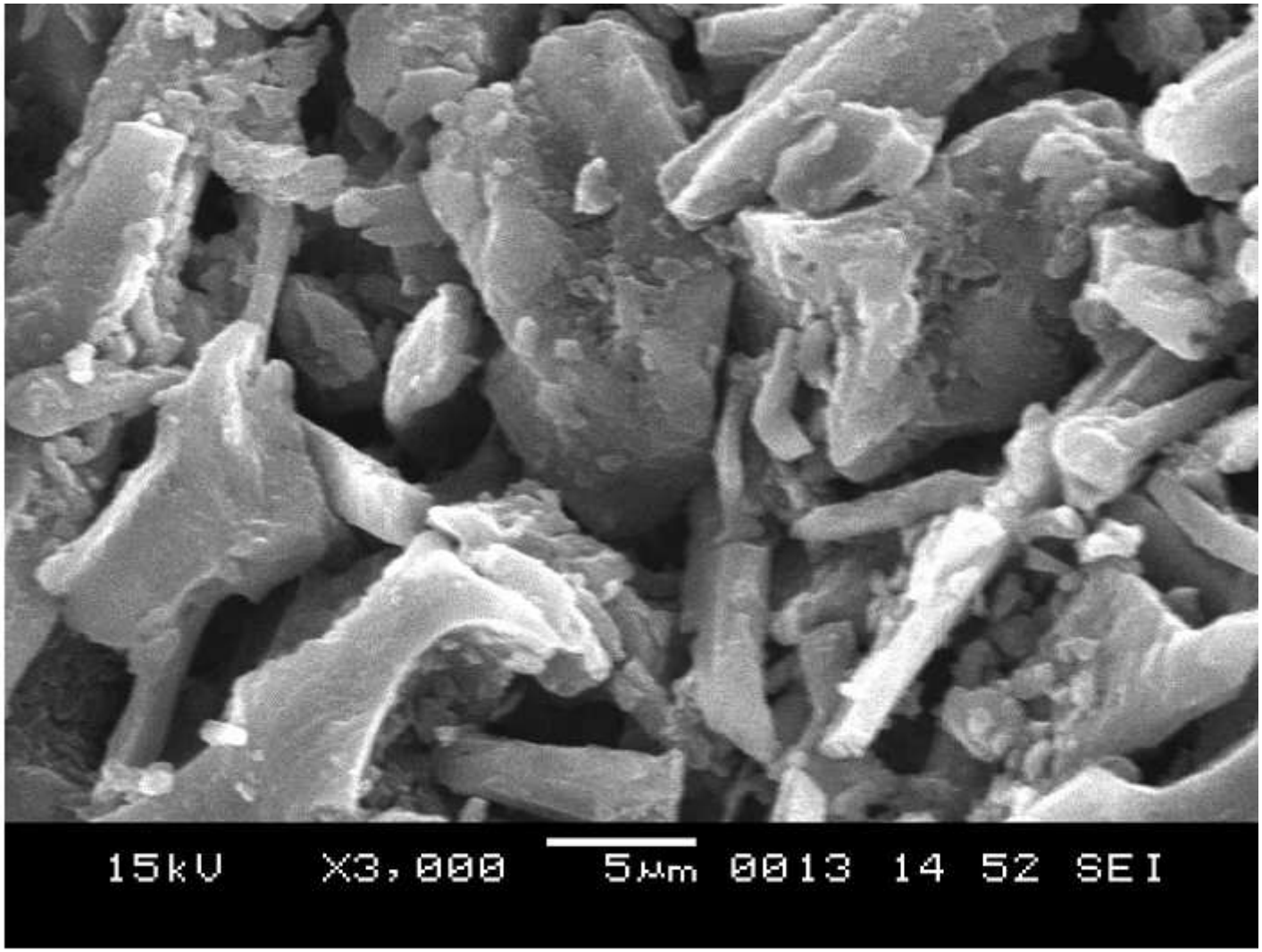

Figure 1

SEM image of Activated carbon

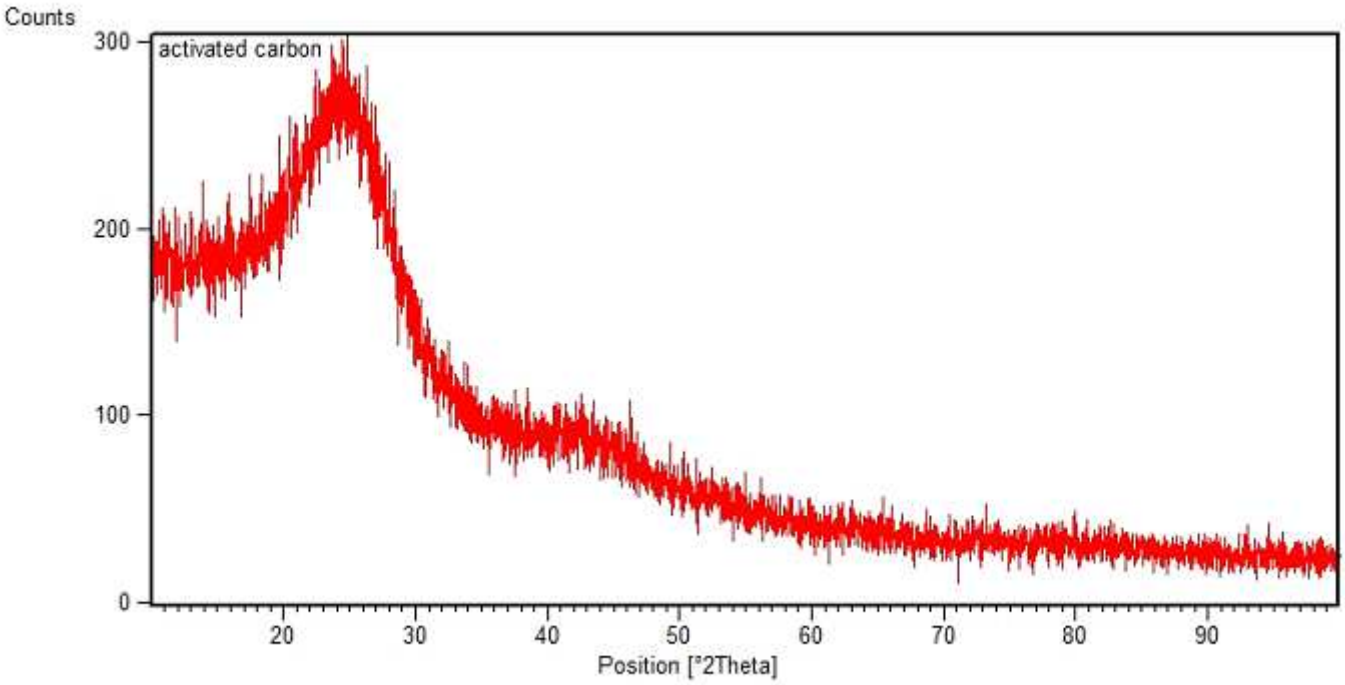

Figure 2

XRD Pattern for Activated Carbon

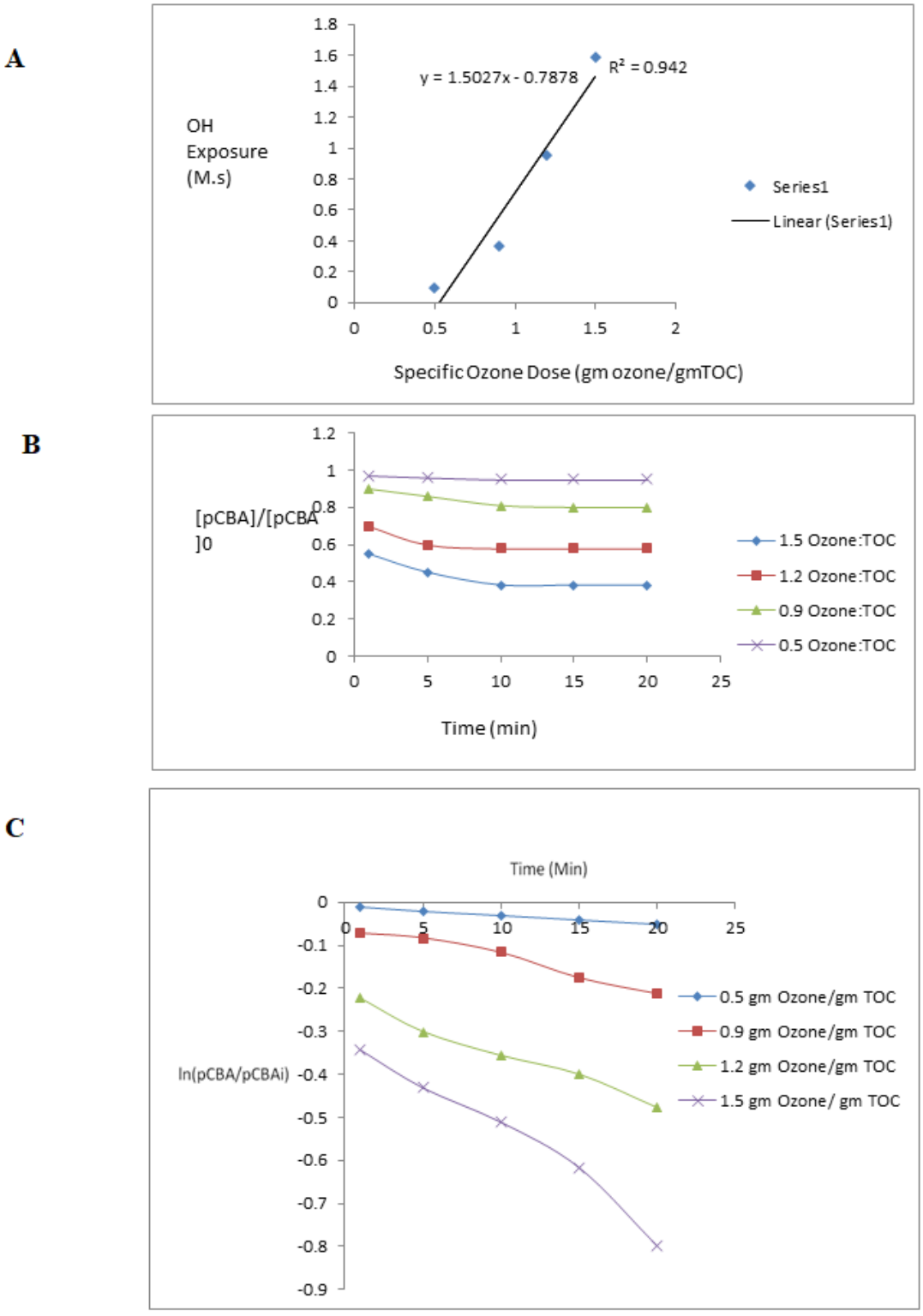

Figure 3

(A) Effect of specific ozone dose on •OH exposure (B) Effect of specific ozone dose on p-CBA degradation (C) Effect of specific ozone dose on rate of p-CBA degradation

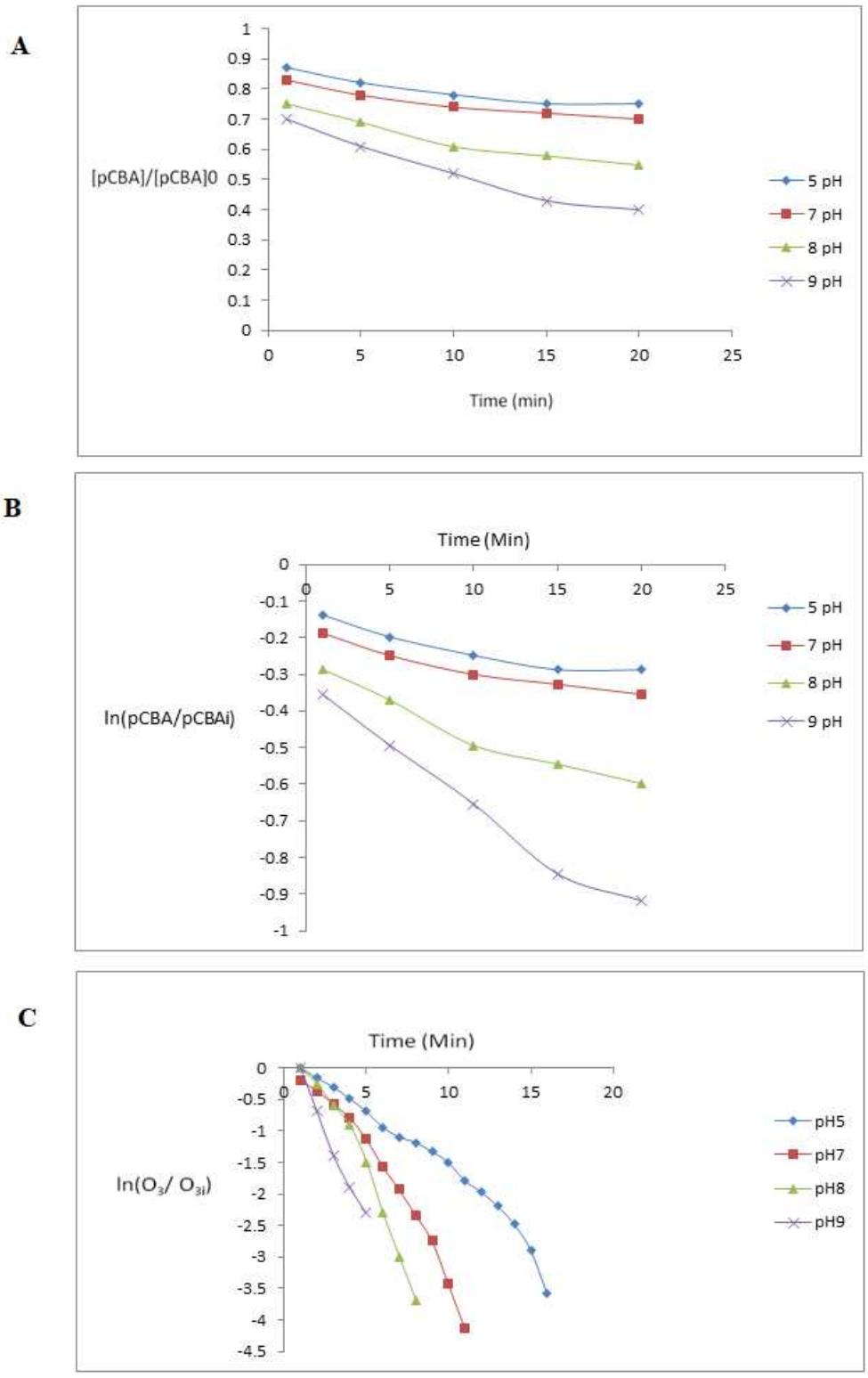

Figure 4

Effect of pH on (A) p-CBA degradation of AC catalyzed ozonation (B) rate of p-CBA degradation of AC catalyzed ozonation (C) rate of ozone decomposition in AC catalyzed ozonation

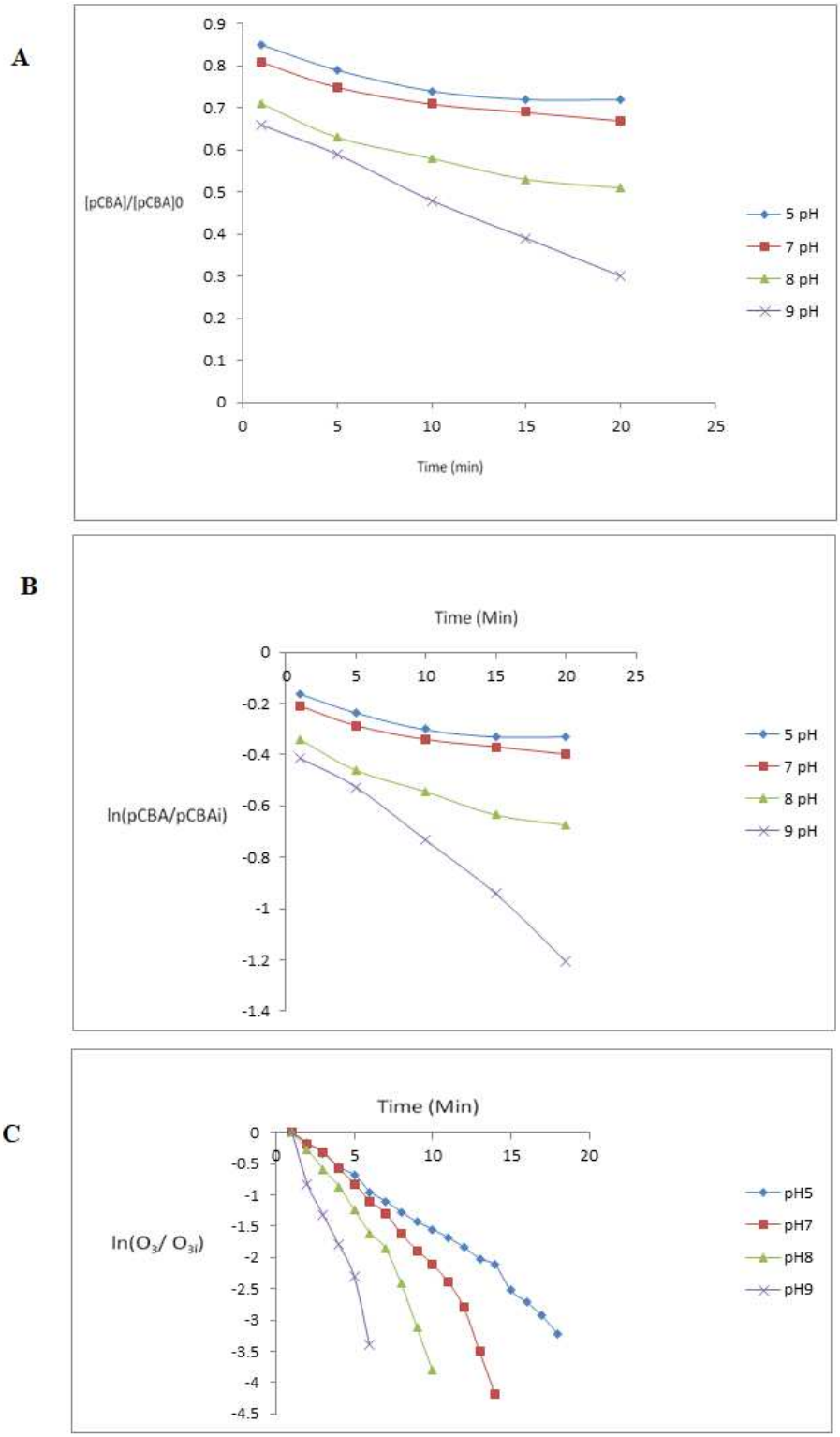

Figure 5

Effect of pH on (A) p-CBA degradation of MWCNTs catalyzed ozonation (B) rate of ozone decomposition of MWCNTs catalyzed ozonation (C) rate of ozone decomposition of MWCNTs catalyzed ozonation

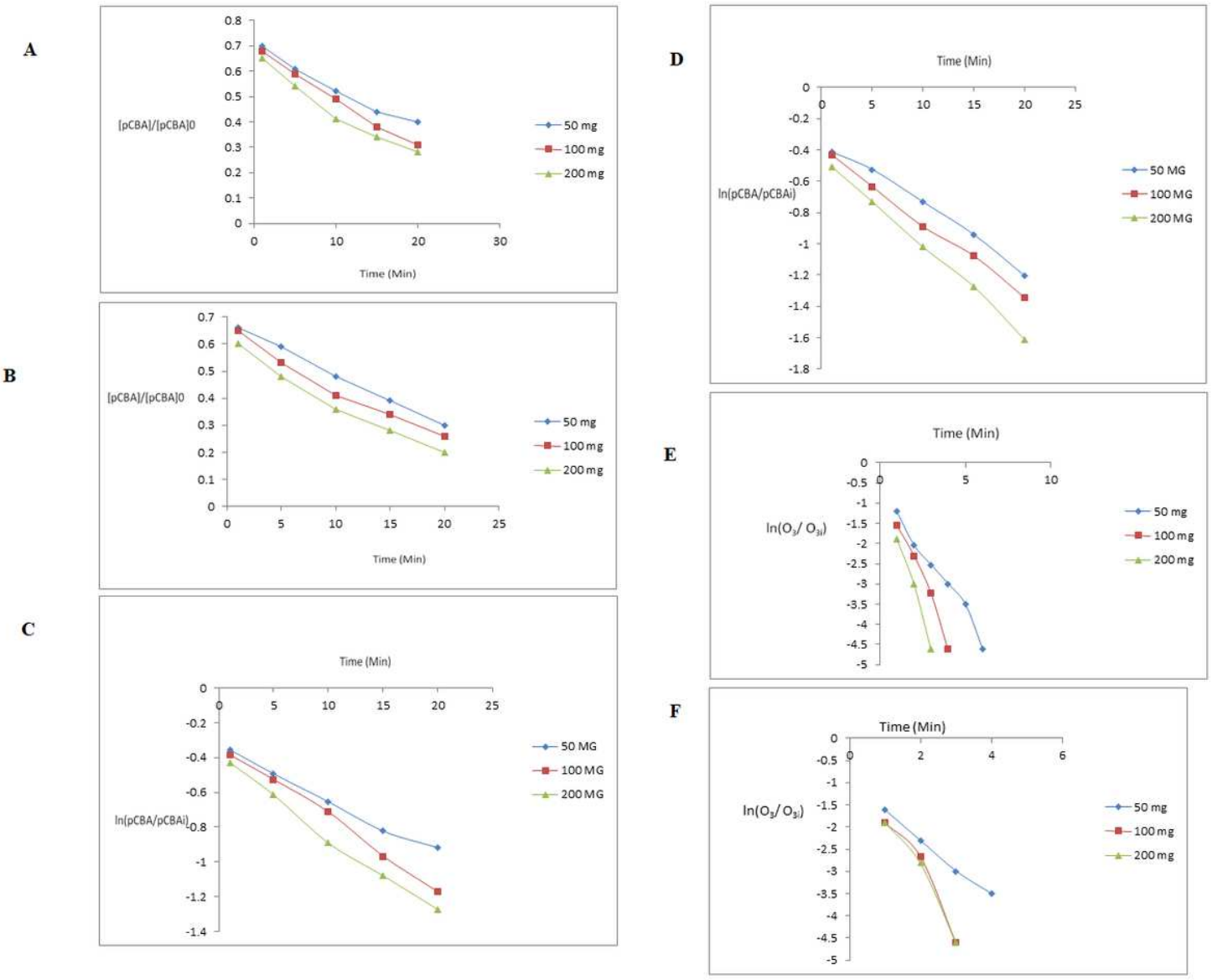

Figure 6

Effect of catalyst loading on(A) p-CBA degradation in AC catalyzed ozonation (B) p-CBA degradation of MWCNTs catalyzed ozonation (C) rate of p-CBA degradation in AC catalyzed ozonation (D) rate of p-CBA degradation in MWCNTs catalyzed ozonation (E) rate of ozone decomposition of in AC catalyzed ozonation (F) rate of ozone decomposition of in MWCNTs catalyzed ozonation

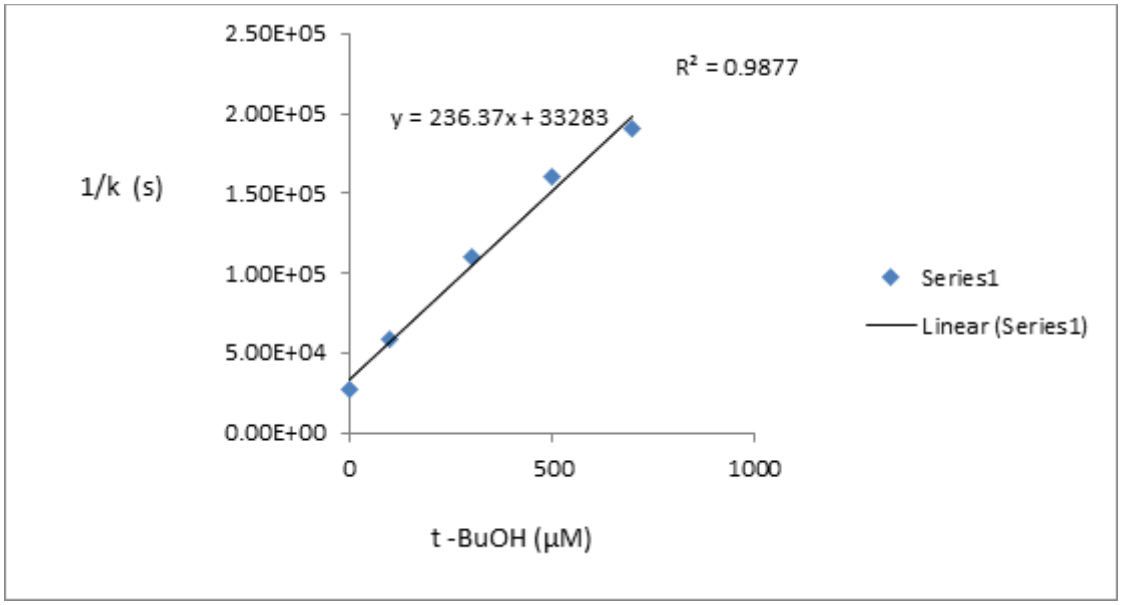

Figure 7

Competition kinetics plot for determination of the 'OH scavenging rate constant

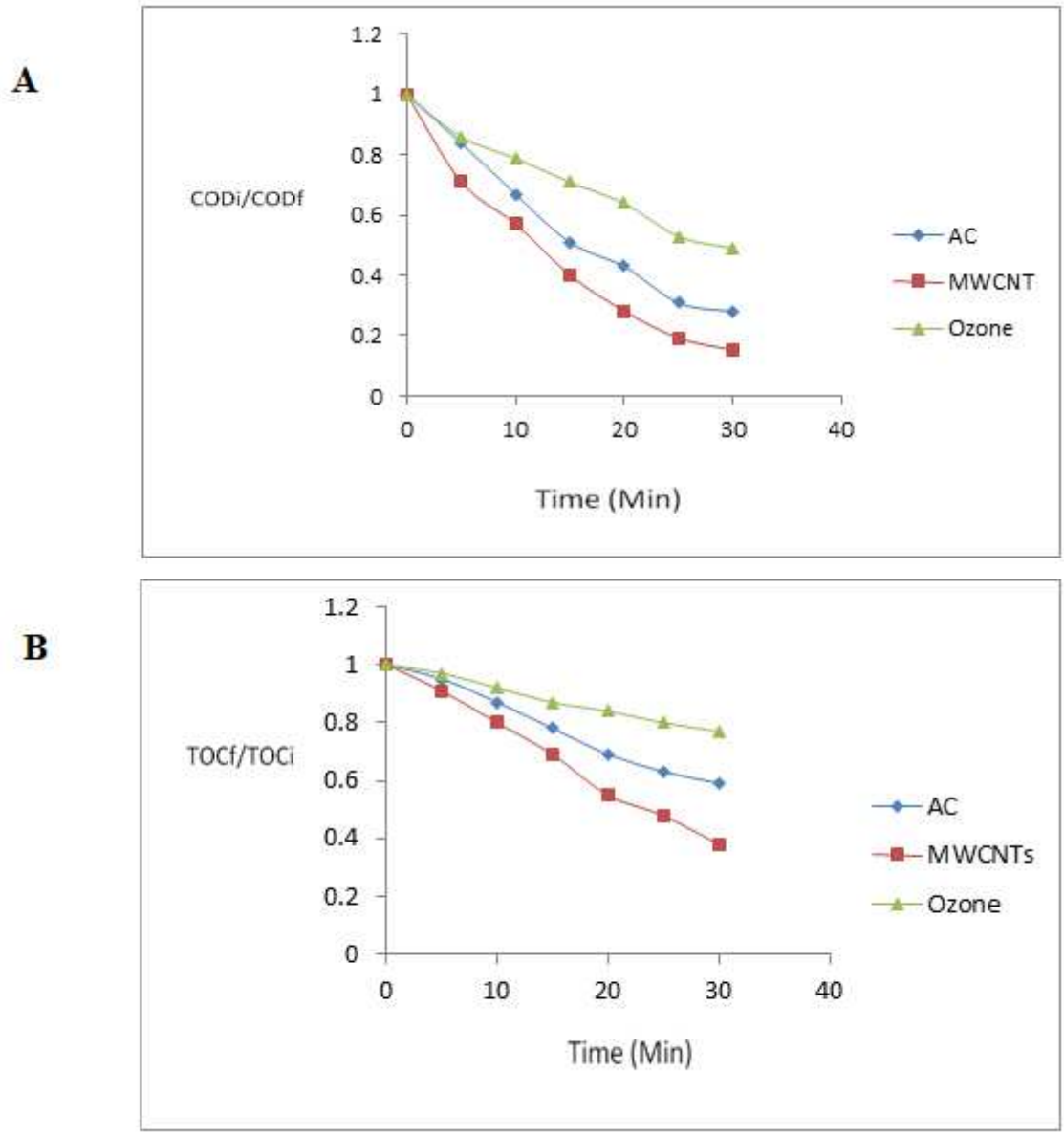

Figure 8

Effect of AC and MWCNT catalyzed ozonation on (A) COD removal (B) TOC removal

Supplementary Files

This is a list of supplementary files associated with this preprint. Click to download.

- GraphicalAbstract.docx